

Temporal Post-Processing in Time-Resolved MR Angiography

Oliver Wieben, Damon Tull

Abstract— This article discusses temporal post-processing strategies to differentiate arterial and venous signal in contrast-enhanced Magnetic Resonance Angiography (MRA). Algorithms were implemented which derive global and local Eigenimages for the suppression of signals from the arteries or the veins. In addition, a regularization procedure is proposed, which smoothes the signal waveforms in the spatial and time dimension. These denoised signals may be used for the segmentation of 4D angiographic data sets in classes such as “artery”, “vein”, and “others”.

Keywords— MR Angiography, Matched Filter, Eigenimages, Regularization, Arterial and Venous Waveforms.

I. INTRODUCTION

THE Vascular Magnetic Resonance Research Group at the University of Wisconsin–Madison recently developed a novel MR angiographic technique, referred to as *3D MR DSA* (Three-Dimensional Magnetic Resonance Digital Subtraction Angiography) [1], [2].

Compared to all other angiographic approaches, *3D MR DSA* is unique in its ability to acquire a series of time-resolved volume images and, therefore, allowing the passage of an injected MR contrast agent to be observed. Time-resolved imaging circumvents problems with synchronizing the timing of the bolus and data acquisition and may potentially increase the diagnostic information obtained in the examination. The reconstructed data volumes for *3D MR DSA* vary, but a typical exam will have 20 to 32 volumes with a resolution of $512 \times 256 \times 32$.

For diagnostic purposes, radiologists are interested in the analysis of the arteries and veins. Therefore, it is desirable to obtain an image with maximum contrast for the signal from the arteries without interference with the signal from veins and vice versa. Typically, 2D projections (so called maximum-intensity-projection (MIP) images as shown in Figure 1) are calculated and displayed, so that the operator or radiologists can choose the time frame of highest diagnostic value. Then, MIP images from different angles are calculated and displayed to reflect the 3D information of the data.

The purpose of this study is the investigation of improvements for *3D MR DSA* in terms of separating arterial and venous signals. In the current implementation, often only 2–3 time frames are used, because they do contain the peak arterial signal. Potentially, the signal-to-noise ratio (SNR) can be improved by incorporating information from all time frames into two final image volumes (arterial only and venous only [3]).

Oliver Wieben is with the Departments of Electrical and Computer Engineering, Medical Physics, and Radiology at the University of Wisconsin–Madison. E-mail: wieben@cae.wisc.edu .

One approach for the separation of the signals is matched filtering. With this approach a signal waveform can be suppressed by properly adjusting weight parameters over the time dimension.

A second approach is based on the segmentation of each voxel. The voxels are categorized as belonging to either an artery, or a vein, or none of the above. Such a segmentation needs “features” which identify the voxels. Such features can be extracted from the signal waveform over time. Since the signal is corrupted with noise, it is desirable to smooth the waveforms to allow for a better feature extraction. In our regularization approach, we denoise the signal by filtering spatially and over time.

II. THEORY

A. Matched Filtering

Matched filtering is one approach to extract specific signals from a set of images. Wang et al. [4] investigated generalized matched filtering to extract (1) signal of the arterial flow and (2) signal of venous flow in time-resolved 2D flow angiography. In this approach, the high temporal resolution of the acquired data allows to differentiate the two signals by the characteristic pulsatility of the arterial blood flow. Filtered images are then generated by a weighted sum of all images in the cardiac cycle. The result were two images: one with optimal SNR for identification of arteries and one for identification of veins.

Wang used human interaction to define regions containing arterial and venous blood. Based on the analysis of these data, coefficients for the weighting coefficients of each pixel $w_k(x, y)$ in the acquired images $s_k(x, y)$ can be determined, so that the resulting image $I(x, y)$ can be calculated as

$$I(x, y) = \sum_{k=1}^K w_k(x, y) s_k(x, y). \quad (1)$$

In this notation, k denotes the time frame number (total number of time frames is K). An undesired signal waveform $\{f_k\}$ can be suppressed in the filtered image $I(x, y)$ by adjusting the weighting coefficients so that

$$\sum_{k=1}^K w_k f_k = 0. \quad (2)$$

The undesired waveform could be the venous waveform $\{v_k\}$ (for an arterial only image) or the arterial waveform $\{a_k\}$ (for a venous only image).

The weighting coefficients are calculated with the Lagrange multiplier method to (a) eliminate signal corresponding to the undesired waveform and (b) maximize the

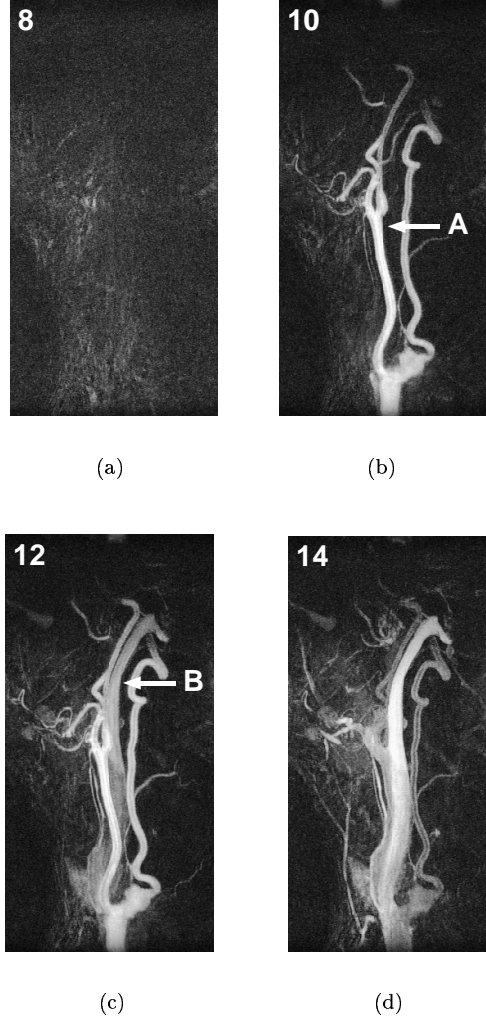


Fig. 1. 3D MR DSA maximum-intensity-projection images for a time series of images obtained from the neck. The series shows sagittal projections at discrete time intervals 8 (a), 10 (b), 12 (c), and 14 (d) during the passage of a contrast agent. The contrast agent has not arrived at time frame 8, but time frame 10 shows a high signal for the carotid artery (A). Image (c) shows the delayed signal enhancement of the jugular vein (B). The length of one time intervals is 5.6 s.

SNR. The Lagrangian multiplier λ is used to construct the Lagrangian

$$L = \text{SNR} - \lambda \sum_{k=1}^K w_k f_k. \quad (3)$$

The task becomes the maximization of L by adjusting w_k while also adjusting λ so that the suppression condition is kept. Therefore, the first derivative of L has to be zero

$$\frac{\partial L}{\partial w_k} = 0, \quad \frac{\partial L}{\partial \lambda} = 0. \quad (4)$$

In these equations, $\frac{\partial L}{\partial w_k} = 0$ is the condition for maximal SNR and $\frac{\partial L}{\partial \lambda} = 0$ is the condition for signal suppression. These equations are then solved for different criteria—such as suppression conditions and maximization criteria.

The image obtained by the matched filter solution depends on the suppression condition and the maximization procedure. A global Eigenimage which optimizes the signal for the waveform $\{f_{\text{opt},k}\}$ is derived by suppressing the signal waveform $\{f_{\text{sup},k}\}$ by means of a global matched filter. The filter coefficients are

$$w_k = f_{\text{opt},k} - (\mathbf{f}_{\text{opt}} \cdot \mathbf{f}_{\text{sup}}) f_{\text{sup},k}, \quad (5)$$

where

$$\mathbf{f}_{\text{opt}} \cdot \mathbf{f}_{\text{sup}} = \sum_{k=1}^K f_{\text{opt},k} \cdot f_{\text{sup},k}. \quad (6)$$

For a local Eigenimage, the filter coefficients vary for the pixels

$$w_k = s_k - (\mathbf{s} \cdot \mathbf{f}_{\text{sup}}) f_{\text{sup},k}. \quad (7)$$

B. Signal Waveforms

An alternative approach to differentiate venous signal from arterial signal is by segmentation of the data set. For this segmentation, each voxel is assigned to one of the three classes “artery”, “vein”, or “background”. Features for the segmentation can be derived from the characteristics of the signal intensity over time for the individual voxels.

In 3D MR DSA, the signatures of the waveforms are not as distinct as for pulsatile blood flow. Figure 2 shows the signal intensities of the carotid artery and jugular vein as obtained from a fast 2D timing scan ($2\text{--}6 \times$ higher temporal resolution as compared to 3D MR DSA). Both signal waveforms can be described as gamma-variant functions

$$s(t) = s_0 t^b e^{(-t/a)}, \quad (8)$$

where t^b describes a function with a high positive slope and $e^{(-t/a)}$ damps the function. The time at which $S(t)$ peaks ($\frac{dS(t)}{dt} = 0$) is at $t = T_p = \frac{b}{a}$. Another characteristic parameter is defined as the mean transit time $T_{\text{mtt}} = \frac{\int S(t)t dt}{\int S(t) dt} = \frac{b+1}{a}$.

C. Deterministic Regularization

The signal for individual voxels is corrupted by noise and not as smooth as shown for the averaged signals in Figure 2. In order to extract suitable features from the waveforms, the data have to be denoised.

Regularized restoration has been widely applied to restore and smooth 2D images [5], [6], [7]. For deterministic regularization prior information about the image is incorporated in the restoration procedure. The problem is formulated as to minimize the Lagrangian

$$\min[\|g - H\hat{s}\| + \alpha \|C\hat{s}\|], \quad (9)$$

where $\hat{s}(x, y)$ denotes the desired estimation of the original (unknown) signal $s(x, y)$, $g(x, y)$ the degraded image, H the distortion matrix, and C a high-pass filter. The high pass filter represents a smoothness constraint for the reduction of high frequency noise. The degree of smoothness

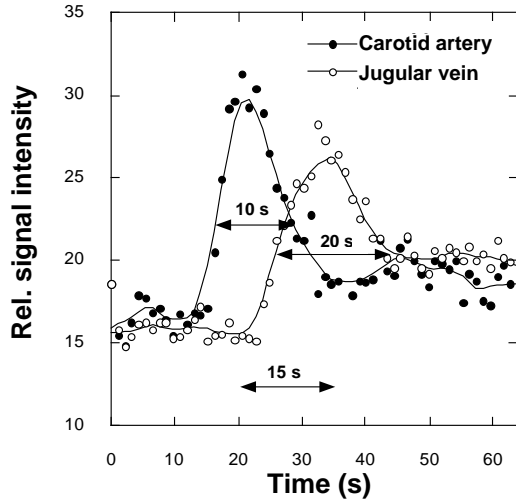


Fig. 2. Plot of the signal enhancement in the carotid artery and jugular vein as a function of time. The data are obtained from averaging signal intensities in a region of interest (ROI) during a 2D timing scan with a temporal resolution of one second. The signal in the carotid artery is characterized by an earlier peak and a faster rising time. The shape of the waveforms can be described by gamma-variant curves and their integral over time is identical.

in the restored image is influenced by the Lagrange multiplier α which is also referred to as *regularization parameter*. Equation (9) can be solved as

$$\hat{s} = (H^T H + \alpha C^T C)^{-1} H^T g. \quad (10)$$

Hunt [5] showed that this restoration can be implemented very efficiently in the frequency domain.

A regularization algorithm can also be applied in one dimension (the time dimension in our case) as

$$\min[\|g_i(x, y) - H\hat{g}_i(x, y)\| + \lambda \|C\hat{g}_i(x, y)\|]. \quad (11)$$

D. Segmentation

Once these estimations are obtained, features such as the peak signal, the peak time, and the peak transit time can be determined. These features can be used for segmentation purposes, which again could help for advanced post-processing (e.g. automatic calculation of vessel-lumen) or visualization methods (e.g. volume rendering or virtual endoscopy). Potential problems for the differentiation between these tissues are the noise in the data and uneven delay times for the filling of the vessels in the image. This may be due to large field of views covered for data acquisition or due to pathologies. However, such a segmentation will not be part of this project but is potential future work.

E. SNR

The signal-to-noise ratio (SNR) is defined in MR imaging as

$$\text{SNR} = \frac{s}{\sigma_N}, \quad (12)$$

where s denotes the signal amplitude and σ_N the standard deviation of the noise [8]. This definition of the SNR is

different from the notation typically used in the signal processing area. The SNR is measured in decibel (dB):

$$\text{SNR}_{\text{dB}} = 20 \cdot \log(\text{SNR}). \quad (13)$$

III. METHODS AND RESULTS

A. Matched Filtering

A 3D MR DSA examination of the carotid artery was used for the calculation of the Eigenimages. The complete 4D data set was normalized to grayscale intensities from 0 to 1. ROIs (≈ 500 voxels) were interactively selected in a slice for an artery and a vein. The waveforms $\{a_k\}$ and $\{v_k\}$ were obtained by averaging the signals in the ROIs from this slice at each time frame. The waveforms were then normalized to $\sum_{k=1}^K f_k^2 = 1$.

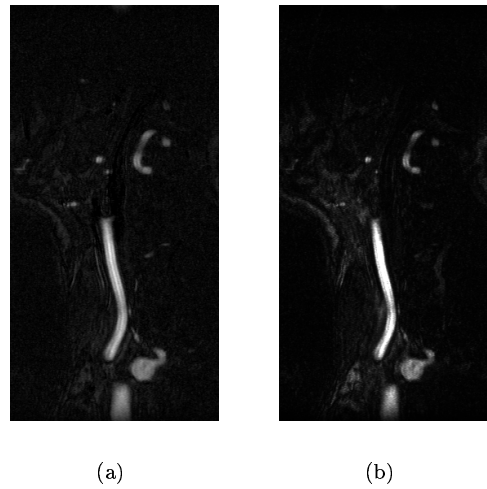


Fig. 3. Global (a) and local (b) arterial Eigenimage of a slice from a 3D MR DSA examination of the carotid artery.

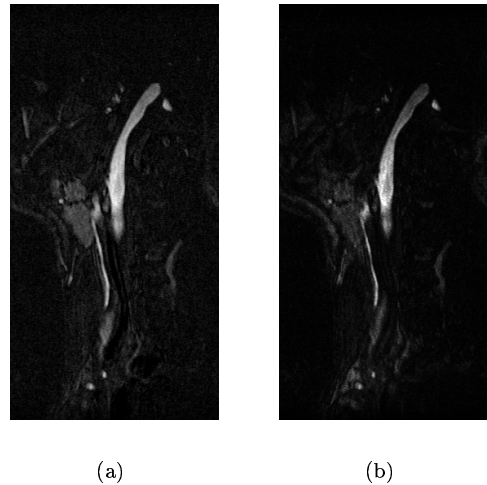


Fig. 4. Global (a) and local (b) venous Eigenimage of one slice from a 3D MR DSA examination of the carotid artery.

The global arterial and venous Eigenimages were calculated as described by equations (1), (5), and (7)). Figure 3

shows the global and local arterial Eigenimage obtained for one slice of the data set. The global and local Eigenimages for optimized venous signal are shown in Figure 4. Gray values outside the range $[0 \ 1]$ have been bounded to stay within the range $[0 \ 1]$.

These Eigenimages have been calculated for each of the 32 slices. 3D image volumes are typically displayed as maximum-intensity-projection images in MR. Such MIP images are shown for sets of global arterial and venous Eigenimages in Figure 5. Each image represents the information from $512 \times 256 \times 32 \times 27$ voxels.

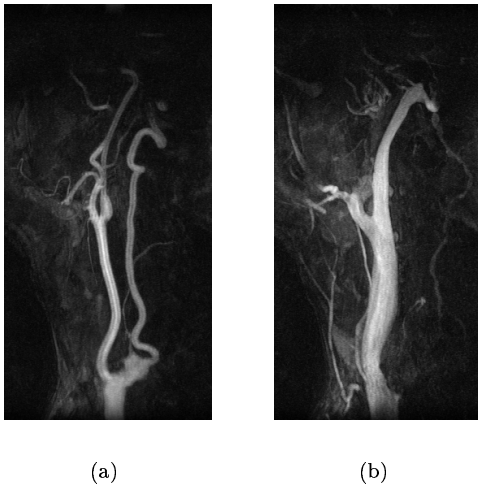


Fig. 5. Maximum-intensity-projection image from the global arterial Eigenimage (a) and the global venous Eigenimage.

The SNR of the MIP Eigenimages was compared to the SNR of a MIP image for one time frame. Time frame 10 from Figure 1 had the highest signal for the arteries with small interference from the veins. Both images were normalized to an interval $[0 \ 1]$. The mean signal for a large ROI was found to be 0.735 and the standard deviation for a large ROI in the air (outside the head and neck) was 0.0165. This corresponds to an SNR of 75.9 dB. The global arterial Eigenimage had an SNR of 78.1 dB (mean signal = 0.732 and $\sigma_N = 0.0147$) for the same ROIs. The experiment was repeated for the MIP venous Eigenimage and time frame 15. In this case the SNR improved from 72.9 dB to 76.7 dB.

B. Regularized Filtering

The smoothing of the data was implemented in two steps. First information about their 2D neighborhood was incorporated and then the data were smoothed as a function of time.

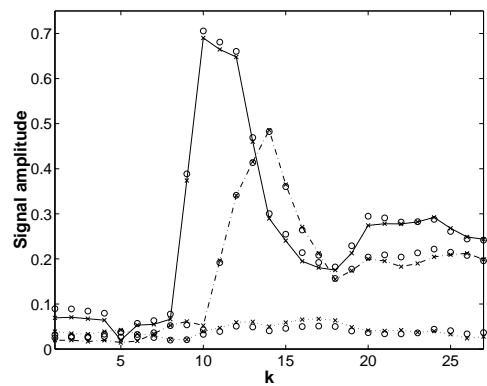
The spatial filtering was implemented according to equation (10). In our case the point spread function $h(x, y)$ was the unit impulse function and, therefore, the Fourier transform H contained a value of 1 in each element. A 2D

Laplacian operator was used for the high pass filter

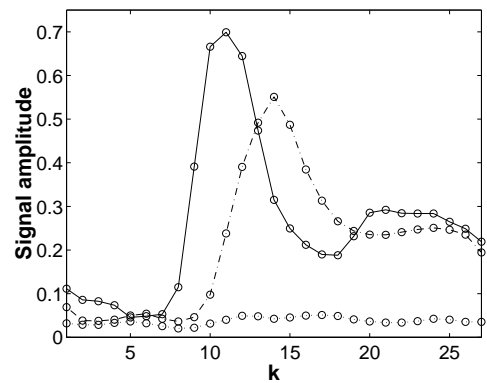
$$C = \begin{bmatrix} 0 & 1 & 0 \\ 1 & -4 & 1 \\ 0 & 1 & 0 \end{bmatrix} \quad (14)$$

The regularization parameter was varied and a value of $\alpha = 10^{-1}$ proved to work well. For a larger α the signal in the vessels becomes more homogeneous but on the other hand the edges get more blurred. Following the spatial filtering, the voxels are filtered as a function of time (see equation (11)). Again, a first order high pass filter was chosen for C ($[1 \ -2 \ 1]$) and α was set to 10^{-1} .

Figure 6 shows signal intensities from representative voxels for an artery, vein, and other tissue. These voxels have been selected interactively and were then analyzed.



(a)



(b)

Fig. 6. Signal intensities of selected voxels as a function of the time frame k . Image (a) shows the acquired data (x) and the data obtained after the regularized filtering (o). The solid line represents a voxel from an artery, the dash-dotted line a voxel from a vein and the dotted line a voxel from other tissue. Image (b) shows the data after an additional smoothing constraint has been applied in the time dimension.

IV. DISCUSSION

The matched filter algorithm allows for the generation of an arterial only and a venous only image. In the illustrated

data set, the obtained angiogram looks similar to the best image from the time series. The SNR increased slightly for the arterial and venous Eigenimages, but the signal from stationary tissues increased as well.

It is also possible to suppress constant signal in the images with a matched filter. This option would remove stationary signal, for example from fat. Typically, stationary signals are removed by the subtraction of a precontrast mask [9]. Potentially, a matched filter may perform better than the mask mode subtraction algorithm.

For the first time, images containing signal from veins only have been produced by the matched filter algorithms. Such images have not been available previously due to the interference with the signal from arteries.

The temporal filtering had by far a bigger impact on smoothing the waveform than the spatial filtering. The 2D high pass filter could have been modified to smooth over more data, but averaging over more data points would have blurred the edges more as well. After applying both regularized filters, the waveform seems to have a more suitable shape for segmentation purposes. Possible features include the ratio of the maximum amplitude over the mean amplitude, the delay of the maximum amplitude and the width of the peak.

A possible extension of the method would be a 3D spatial filtering and a temporal filtering. This approach may not add too much value though, because the spatial filtering in 2D did not seem to change the waveform of the data very much.

The segmentation itself remains a future task too. Various approaches for segmentations have been proposed in the literature, for example statistical approaches, neural networks, fuzzy logic systems etc.

ACKNOWLEDGMENTS

The author would like to acknowledge the suggestions of Professor Damon Tull, even though he has not been able to implement all of them. This may leave some opportunities for motivated students who search for a Ph.D. thesis project.

REFERENCES

- [1] F. R. Korosec, R. Frayne, T. M. Grist, and C. A. Mistretta, "Time-resolved contrast-enhanced 3D MR angiography," *Magnetic Resonance in Medicine*, vol. 36, pp. 345–51, 1996.
- [2] R. Frayne, T. M. Grist, F. R. Korosec, D. S. Willig, J. S. Swan, P. A. Turski, and C. A. Mistretta, "MR angiography with three-dimensional MR digital subtraction angiography," *Topics in Magnetic Resonance Imaging*, vol. 8, pp. 366–88, 1997.
- [3] R. Frayne, "Time-resolved contrast-enhanced 3D MR angiography," Whitaker foundation research grant, University of Wisconsin-Madison, Depts. of Medical Physics and Radiology, 1996.
- [4] Y. Wang, D. M. Weber, F. R. Korosec, C. A. Mistretta, T. M. Grist, J. S. Swan, and P. A. Turski, "Generalized matched filtering for time-resolved MR angiography of pulsatile flow," *Magnetic Resonance in Medicine*, vol. 30, pp. 600–8, Nov. 1993.
- [5] B. R. Hunt, "The application of constrained least squares estimation to image restoration by digital computer," *IEEE Transactions on Computers*, vol. C-22, pp. 805–812, Sept. 1973.
- [6] R. C. Gonzales and R. E. Woods, *Digital Image Processing*. Reading, MA: Addison-Wesley, 1992.

- [7] M. R. Banham and A. K. Katsaggelos, "Digital image restoration," *IEEE Signal Processing Magazine*, vol. 14, pp. 24–41, Mar. 1997.
- [8] D. G. Nishimura, *Principles of Magnetic Resonance Imaging*. Stanford, California: Stanford University Press, 1996.
- [9] C. A. Mistretta and A. B. Crummy, "Diagnosis of cardiovascular disease by digital subtraction angiography," *Science*, vol. 139, pp. 761–5, 1981.

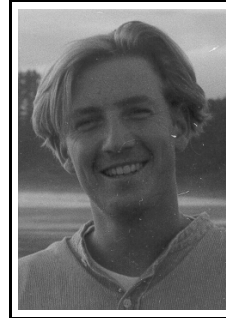


Fig. 7:

OLIVER WIEBEN received his Vordiplom in Electrical Engineering at the Universität Hannover, Germany in 1993, his Diplom at the Universität Karlsruhe, Germany in 1998 and his MS degree at the University of Wisconsin, Madison in December 1996, where he is a Ph.D. student in Electrical and Computer Engineering by now. His research is related to biomedical engineering applications involving digital signal processing, image processing, and pattern recognition. He contributed to the development of the MEET-Man Project at the Universität Karlsruhe, where a detailed finite element model of the human body was created based on tissue-classified MRI scans. The work for the MS thesis focussed on automated ECG interpretation (such as beat detection and classification) with a filter bank approach. His current research at the Departments of Medical Physics and Radiology is related to medical imaging. He wants to improve time resolved and contrast enhanced 3D Magnetic Resonance Imaging. In particular, he is developing a fast and interactive system for reconstructing and displaying 'preview' images of high quality for the operators and radiologists. Mr. Wieben is a member of the Institute of Electrical and Electronics Engineers (IEEE), the American Association of Medical Physicists (AAMP), and the International Society for Magnetic Resonance in Medicine (ISMRM).